Key Engineering Materials
ISSN: 1662-9795, Vol. 926, pp 1051-1060
doi:10.4028/p-d09adu

Submitted: 2021-12-09
Revised: 2022-01-25
Accepted: 2022-02-04
Online: 2022-07-22

A Critical Evaluation of Forming Limit Curves Regarding Layout of Bending Processes

Peter Frohn-Sörensen[1,a*], Daniel Nebeling[1,b], Jonas Reuter[1,c] and Bernd Engel[1,d]

[1]Chair of Forming Technology at the University of Siegen, Breite Strasse 11, 57076 Siegen, Germany

[a]Peter.Frohn@uni-siegen.de, [b]Daniel.Nebeling@uni-siegen.de, [c]jonas.reuter@uni-siegen.de, [d]bernd.engel@uni-siegen.de

Keywords: FLC, Failure Criterion, Necking, Profile Bending, Flexibility, kinematic forming

Abstract. Forming limit curves (FLCs) are important to predict failure against biaxial deformation in sheet metal forming. Particularly crucial is the detection and evaluation of the stable/instable transition which indicates necking and ultimately leads to rupture. In the past, it has been observed that specific processes, in particular free-form bending processes, might not be predicted well by conventionally evaluated FLCs, i.e. the Nakajima experiment, where tapered sheet metal specimens are stretched over a hemispherical punch until material failure. In the present study, FLCs are evaluated from such Nakajima tests and from notched tension tests (NTT) highlighting large differences in between both results. The differences in between the evaluation methodologies are discussed with respect to contact and bending strain in the forming zone. The FLCs of three tested sheet metal materials are compared to fracture strain resulting from an incremental bending process with free forming zone demonstrating an increased failure prediction accuracy by the NTT FLCs than by the conventional ones. In the light of these results, it is therefore encouraged to critically assess the application of FLCs obtained from NTTs to various free-form bending processes.

Intoduction

Forming limit curves (FLC) evaluated by standardized laboratory experiments such as Nakajima are widely used to characterize failure against necking in plane stress state according to [1]. The FLC is hence applied to determine failure in sheet metal forming. Out of a wide variety of testing methods for the determination of the FLC or parts of it, the NAKAJIMA testing procedure standardized in DIN EN ISO 12004-2 is the most commonly used [2]. Specimens with different tapered widths reveal specific plane stress conditions when stretch drawn over a hemispherical punch in a test assembly according to [3]. During plastic stretching, the tapering width of the specimens affects minor strain and, hence, strain ratio ρ, which is defined as the ratio between major and minor strains. Ideally, therefore a variation of width is selected in a way to cover the whole span of the FLC in between uniform biaxial strain up to uniaxial strain. Thorough lubrication of the experiment in between punch and specimen is crucial to reduce the influence of friction on the material deformation as much as possible. Different lubricants are applied, ranging from oils and greases, as suggested by the technical standard, up to Teflon films which have been used by [4]. This approach to quantifying the forming limit of a given material usually allows accurate prediction of conventional forming processes with a high degree of geometric relation between tool and product, to the extent that the tool already contains the final geometry of the forming operation. Particularly, in profile bending, FLCs were successfully applied to layout rotary draw bending processes [5]. When it comes to kinematic bending processes, flexibility is often achieved by a universal tooling approach, where the process parameters define products geometry rather than the shape of the tools [6]. This feature leads to very limited contact areas of tools and profiles resulting in a free forming zone [7]. Due to the lack of lubrication, friction and direct contact in the forming zone of such processes, a failure prediction by FLCs evaluated from tool bound experiments such as Nakajima has proven complicated in past [8].

Material Characterization and Modelling

Technical material properties. A variation of three high-strength sheet metals is regarded, namely the boron manganese steel 22MnB5 commonly used for hot stamping applications, a dual-phase steel HCT780X "DP800" which is widely used in automotive stamping applications and a novel austenitic steel pre hardened by cold rolling. The mechanical material parameters were determined by uniaxial tensile tests according to DIN EN ISO 6892-1 using the specimen geometry suggested in DIN 50125 with a parallel length of l_0 = 80 mm. The resulting material parameters are summarized in Table 1.

Table 1: Mechanical material parameters obtained from tensile tests.

Material	s_0 [mm]	R_e [MPa]	R_m [MPa]	n [-]	ε_f [%]
HCT780X	1.5	487	774	0.124	19
22MnB5	1.4	339	509	0.113	22
FORTA H800	2.0	734	975	0.262	38

Analytical modelling of the forming limit curve. A common method for modelling the FLC is the semi-analytical method of KEELER [9], next to approximations, such as the numerical approaches of [10] and [11]. The most important models are summarized by [12]. KEELER's semi – empirical formulations were developed on the base of experiments on ductile deep drawing steels (R_e ranging from 217 up to 628 MPa), aluminum, brass and copper alloys [4, 13]. The resulting model takes the initial sheet metal thickness s_0 and its hardening exponent n into account, next to empirical factorizations. In KEELER's approach, the FLC is described by the parameter of limiting strain FLD_0 which follows

$$FLD_0 = \ln\left[1 + \left((23.3 + 14.13 \cdot s_0)\frac{n}{0.21}\right)/100\right]. \quad (1)$$

according to HORVATH [14]. Keeler's FLC equation is valid up to a sheet thickness of s_0 = 3.1 mm [15]. FLD_0 applies at plain strain conditions ($\varphi_2 = 0$). Regarding the trend of the FLC in the first and second quadrant of the FLD, KEELER provided a case distinction for the curve following

$$\varphi_1 = -\varphi_2 + FLD_0 \quad (2)$$

for $\varphi_2 < 0$ and

$$\varphi_1 = 0.2 \cdot \varphi_2 + FLD_0 \quad (3)$$

for $\varphi_2 > 0$.

The FLC model of KEELER is parameterized by the mechanical material properties evaluated in tensile tests. According to eq. (1), the KEELER FLC is parameterized by initial sheet metal thickness s_0 as well as the hardening exponent n. The FLC approximation models the knee of the curve at plane strain ($\varphi_2 = 0$), which, hence representing a material's sensitivity against forming under plane stress conditions. At this strain ratio, the KEELER's FLC supports on *FLD0*.

Determination of FLCs by Nakajima experiments. For determination of a FLC, the technical standard DIN EN ISO 12004-2 suggests the NAKAJIMA test assembly according to [3, 4, 9]. A factor 2 downscaled assembly is utilized which also means reducing the specimen dimensions. Because the original test assembly is suggested being valid up to an initial blank thickness s_0 of 4 mm for reasons of superposed bending strain over the hemispherical dome punch, the assembly is assumed valid for $s_0 \leq 2$ mm. In this paper, forming of ultra- and advanced high-strength steels is focused.

A range of tested strain ratios is achieved in the experiment by varying the specimens' tapering width. Because no specific widths are explicitly suggested by DIN EN ISO 12004-2, the following specimen widths have been chosen based on the experience of previous FLC studies on this test assembly [16]: 100 mm square specimens as well as tapering widths of 65 mm, 50 mm, 40 mm and 25 mm. If necessary, additional specimens were added to cover a larger range within the FLD (15 mm in the case of HCT780X). The specimens were extracted by micro water jet cutting and carefully sanded on their edges. Next, they were gridded electrolytically on their surfaces to facilitate optical strain measurement (OSM) during NAKAJIMA tests.

The NAKAJIMA test includes procedure as described in DIN EN ISO 12004-2. For all material tests, friction was optimized by lubricating with grease and deep drawing foil between stamp and specimen. Hereby, permissible strain maxima were obtained, judged by less than 15% offset from the apex of the punch's dome. Each pair of major and minor strain at failure will deliver a supporting point for the FLC according to the specimens' widths. To capture strain throughout the experiment, the VIALUX AUTOGRID system is attached to the NAKAJIMA test assembly. From the recorded test sequence, the last frame before visible necking (or cracking for brittle materials) occurred is chosen for evaluation.

DIN EN ISO 12004-2 suggest a location-based evaluation of the FLC tests. Perpendicular to the strain maximum's extension on the blank surface, five line cuts were evaluated by means of strain over grid length. Potentially, a very coarse maximum is obtained due to material localization and is therefore interpolated by a polynomial function. The supporting points of this function are found at the zeroes of the second derivation of major strain $\ddot{\varphi}_1$ next to the crack. The vertex of the polynomial function delivers the value of major strain, while minor strain is obtained directly from the line cut. For each supporting point of the FLC, seven test repetitions for the statistical evaluation of major and minor strain were pursued.

Figure 1 shows the obtained FLCs in the φ_1 - φ_2 area. With respect to the specimen width, the mean FLC is calculated from the repetitions (five at least) of each individual tests.

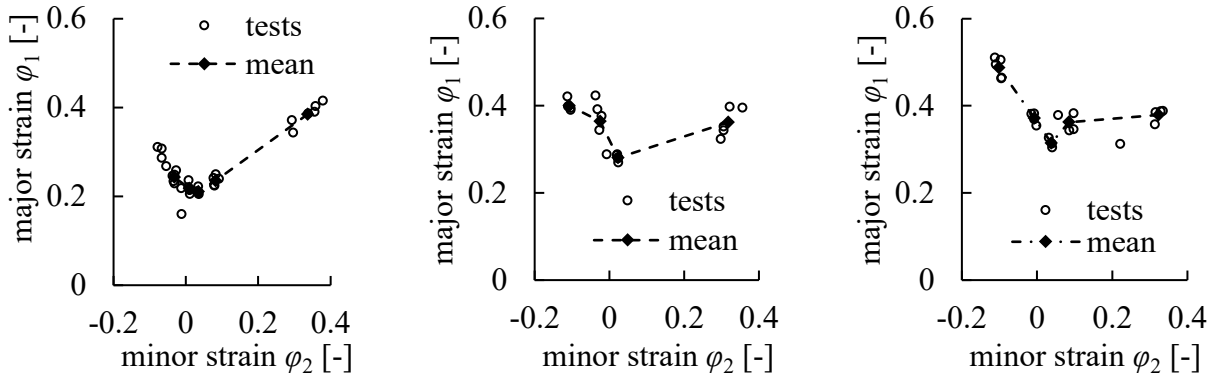

a) HCT780X, s_0 = 1.5 mm b) 22MnB5, s_0 = 1.4 mm c) FORTA H800, s_0 = 2.0 mm

Figure 1: Experimentally determined forming limit curves for a) HCT780X, b) 22MnB5, c) FORTA H800. All curves were tested on a1:2 scaled NAKAJIMA test assembly.

Distinct FLCs are obtained from the testing method. The global average scatter with respect to materials and specimen widths allows to determine strain with a standard strain deviation of 0.015. Most specimens failed well within the margins of max 15% offset to the spherical dome's apex. The FLC minima of all materials are slightly shifted toward positive φ_2 values.

In the cases of HCT780X and 22MnB5 the biaxial tension specimens reveal significantly higher scatter (s = 0.025), than the other tapered widths. An explanation could be, that tapered specimens give the experiment a favored directionality for failure perpendicular to the tapered length, which occurs at similar locations, depending e.g., on friction influences. This hypothesis agrees with the observations of [10], who concluded that necking would appear perpendicular to a predominant major

strain. A square or circular specimen has no directionality which potentially adds to the area of failure possibility and, hence, spread of results.

Determination of FLCs by notched tension tests (NTT). In addition to NAKAJIMA'S experimental procedure, a second approach for testing failure limit curves was conducted for the sheet metal materials HCT780X, 22MnB5 and FORTA H800. Similar to the specimens' tapering width variation, which causes distinct strain ratios to occur in the NAKAJIMA experiment, notched tensile test specimens allow to differ the obtained relation of major and minor strain by varying the notching radius according to [17].With notched tensile experiments, forming limits in the second quadrant, i.e. negative minor strain, are tested [18]. A crucial difference to the NAKAJIMA approach lies in the absence of the influence of friction or lubrication on the experiment, similar to hydraulic bulging [1]. Moreover, the normal pressure applied by the punch in the NAKAJIMA experiment as well as heat transfer from the forming zone in the sheet metal towards punch is missing in notched tensile tests. By the notched tension tests, a closer similarity to profile forming is pursued because of the free forming zone without tool contact.
From the sheet metals considered in the present work, notched tensile specimens were manufactured with a taper width of 10 mm and notch radii varying in between 2.5, 5, 10, 20 and 40 mm. The specimens were painted with a stochastic pattern in order to be ready for optical strain measurement by GOM ARAMIS, see Figure 2 a). The camera-based system dynamically measures spatial coordinates, displacements and surface strain based on the physical principle of triangulation. For the experiments, the notched samples were clamped in the uniaxial testing machine Zwick/Roell Z250 and subjected to tensile elongation. Their deformation was captured at the surface of each specimen by the ARAMIS system (b) with a frame rate of 2 Hz. Each specimen geometry was tested in three repetitions.

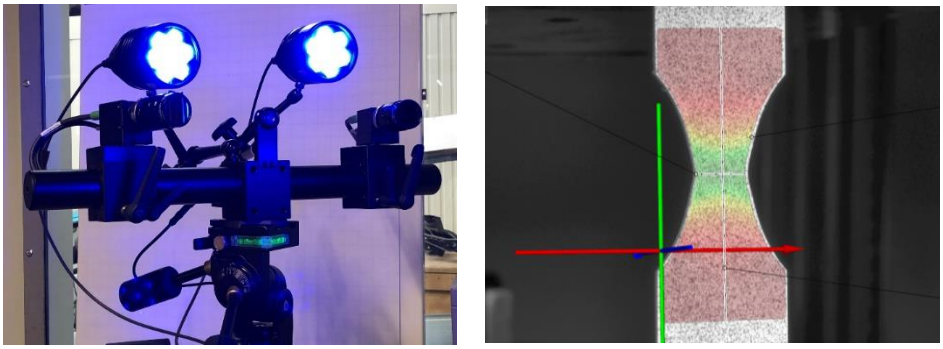

a) b)

Figure 2: Testing notched tensile specimens. a) gom ARAMIS main assembly, b) major strain resulting from testing a radius 20 mm notched specimen (red to green ranging from $\varphi_1 = 0$ to 0.5).

The ARAMIS system (Adjustable Base 12M) was calibrated with at measurement volume of 170x130x80 mm^3 resulting in a local resolution of 23.7 pixel/mm. The facet size is 19 pixels and the point distance 16 pixels. The default strain calculation method implemented in the software GOM CORRELATE was used to evaluate true surface strains of the NTT specimens.
For software evaluation, longitudinal and lateral sections were arranged in the deformation zone of each specimen. The averages, minima, maxima, and standard deviations of the captured major and minor strain gradients were calculated within these sections and exported over the experimental progression, synchronized with the force channel of the testing machine. From these data, the failure limit value within the FLD is investigated.
While the evaluation of failure from measurements obtained from notched specimens follows no standardized procedure, for FLC tests according to NAKAJIMA a variety of approaches is known for determining the transition from stable deformation towards instable necking. The location-based approach defined in DIN EN ISO 12004-2 evaluates major and minor strain trends plotted over a section, which is placed perpendicular to the evolving crack. Under neglect of progression, the

evaluation is conducted at the very frame, captured when the first sign of necking is discernible by the unaided eye. In contrast, time-dependent approaches were suggested, such as by [19]. For a distinct coordinate placed at the area of maximum deformation, the major strain trend over time is evaluated. Their theory defines, that distinct constant inclinations exist in the areas of stable and instable deformation, respectively. Hence, the transition is located by two linear fits at the beginning and end of the first derivation of strain, i.e., major strain rate φ_1', plotted over time. In addition, [20] suggest considering the coefficient of determination applied to the second derivation of strain over time in order to provide an independent and automatable evaluation method for the determination of a stable-instable transition for a given FLC experiment.

As a very basic method applied to standard tensile testing specimens according to DIN EN ISO 6892-1, the maximum of force over time is considered as first approach for evaluating the notched tensile experiments of this paper. The pair of major and minor strain values corresponding to this force maximum F_{max} criterion is determined for each specimen from the averages of the lateral section (cf. Figure 2 c). In addition, the above-described methods are applied to the notched tensile experiments to evaluate the FLCs from the regarded sheet metal materials.

The resulting strain paths from the notched tensile experiments are displayed for HCT780X in Figure 3 a). For all materials, these paths range in between plain strain ($\varphi_2 = 0$) and uniaxial tension ($-2\ \varphi_2 = \varphi_1$) in the FLD. Larger radii deliver lower minor strain values while smaller radii would lie closer to plain strain. Steeper inclinations of the strain paths are observed for higher major strain values. In the GOM ARAMIS software, the longitudinal section is utilized to identify the location of maximum strain and, subsequently, material failure due to cracking. At this position, the data from the lateral section are used for further processing. Considering these data, a significantly higher spread of major and minor strain values is observed for smaller notch radii.

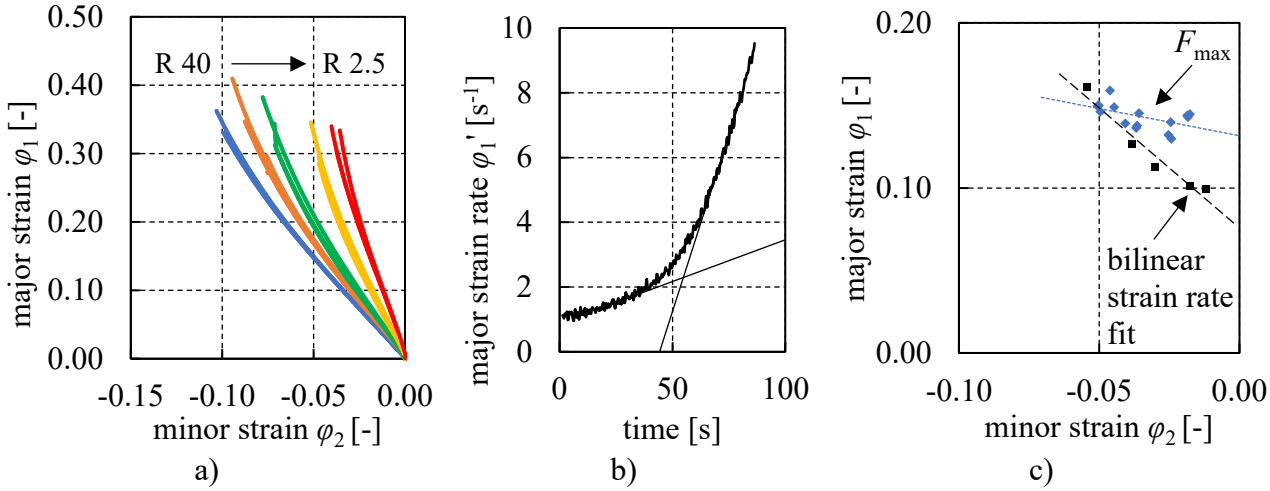

Figure 3: FLC evaluation from notched tensile specimens. a) FLD plot of all experiments on HCT780X with colors corresponding to distinct notch radii ranging from 40 to 2.5 mm, b) evaluation of stable-instable transition by a bilinear fit to strain rate over time for a R 10 mm specimen, c) linear FLC interpolations, resulting from different evaluation methods.

In order to extract FLCs from the experiments, for each dataset corresponding to an individual specimen the timestep of maximum force F_{max} is regarded to obtain the major/minor strain data pairs form the section's average. Moreover, the method of VOLK and HORA is applied [19]. After calculating the first derivation of strain over time, $\dot{\varepsilon} = \frac{\partial \varepsilon}{\partial t}$, two distinct areas of strain rate over time are identified, where a constant inclination of the trend is valid. Fitting and extrapolating linear functions in these areas delivers the location of the stable-instable transition (see Figure 3 b). Regarding the present investigations, the VOLK/HORA method is applicable to all experiments on notched tension tests.

Incremental Swivel Bending (ISB)

For comparison of the evaluated FLCs according to the NAKAJIMA procedure, and, as evaluated from notched tension tests, an incremental in-plane bending method is conducted on the materials introduced in this paper. Incremental Swivel Bending (ISB), as presented by Engel et al. [21], offers the opportunity to successively increase the number of overlapping increments so that longitudinal strain at the extrados of a bent profile converges towards the forming limit due to cracking. In principle, the ISB method consist of two equally loaded clamping units of which one pivots about the bending axis of the tool [8]. The bending moment is transmitted by friction under the clamping units, thus resulting in a forming zone which relates to the gap opened in between the clamping units but also to the material portion drawn out of the clamping [22]. Notably, even though the material is clamped firmly under dry static friction conditions at high surface pressure [23], the material loses contact to the tools as soon as reaching its yield point. Thus, a free forming zone without tool contact is obtained corresponding to free-form bending methods, which shall be compared to the FLC evaluation methods presented in this paper.
For the present paper, flat material strips of 50 mm width were incrementally bent in-plane. The incremental feed Δf in between the formed increments was decreased successively until failure according to the experimental procedure summarized in Table 2. The material strips were subjected to bending in a way that the strain neutral fiber lies at the intrados of the arc resulting in a linearly increasing tensile strain distribution. This approach avoids compressive strain at the intrados and, therefore, the formation of wrinkles.

Table 2: Processing parameters of incrementally bent sheet metal strips.

Material	s_0 [mm]	F_N [kN]	δ [°]	Δf [mm]
22MnB5	1.4	500	3.25	{100…3}
HCT780X	1.5	816	5.25	{123…12}
FORTA H800	1.0	900	6.25	{110…3.5}

Afterwards, the resulting strain gradients were evaluated from the surfaces of the bending specimens. In detail, strain maps were captured by optical strain measurement on a VIALUX AUTOGRID system calibrated to a quadratic grid pattern with 2 mm nominal grid length. The grid marking was applied to the bending specimens prior to ISB by electrolytical etching. From the strain maps of the forming zones of the bent strips, major and minor strain values were measured as maximum values at the outer fiber to be compared to the FLCs. Linear strain paths were observed from the incremental superposition.

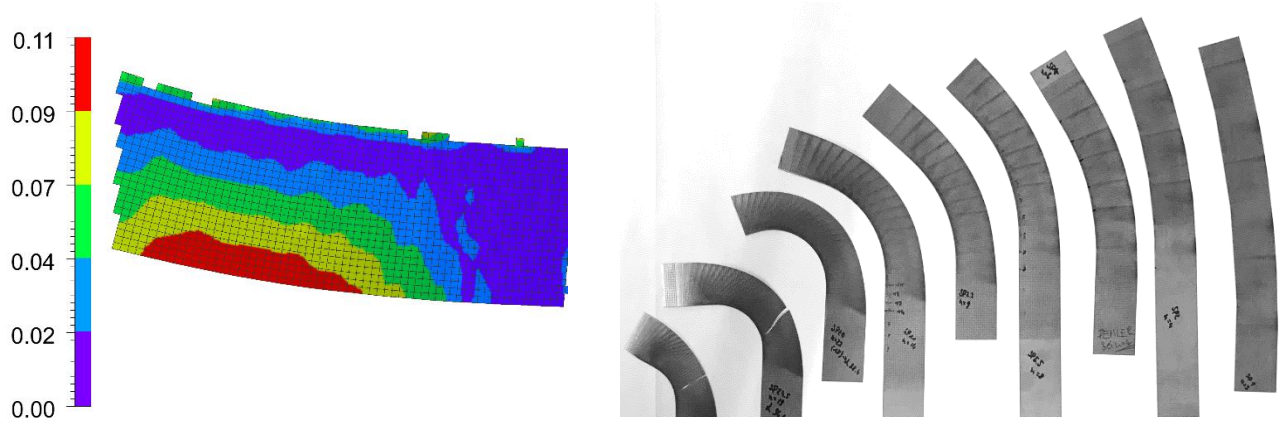

a) b)

Figure 4: Incremental in-plane bending of flat material strips with successively increasing strain. a) strain map obtained from FORTA H800 with an incremental feed of Δf = 7 mm and b) incremental bending series of FORTA H800.

Results

For three different high-strength sheet metals, the model-based KEELER FLC approximation is compared to the experimental procedures according to NAKAJIMA as well as notched tension tests (NTT). All of these failure predictions within the major-minor strain plane assume linear strain paths resulting from forming. Moreover, an incremental bending method is compared with successively decreasing incremental feed which results in a stepwise increase of strain. All experiments and FLCs are plotted in one individual graph for each material in Figure 5.

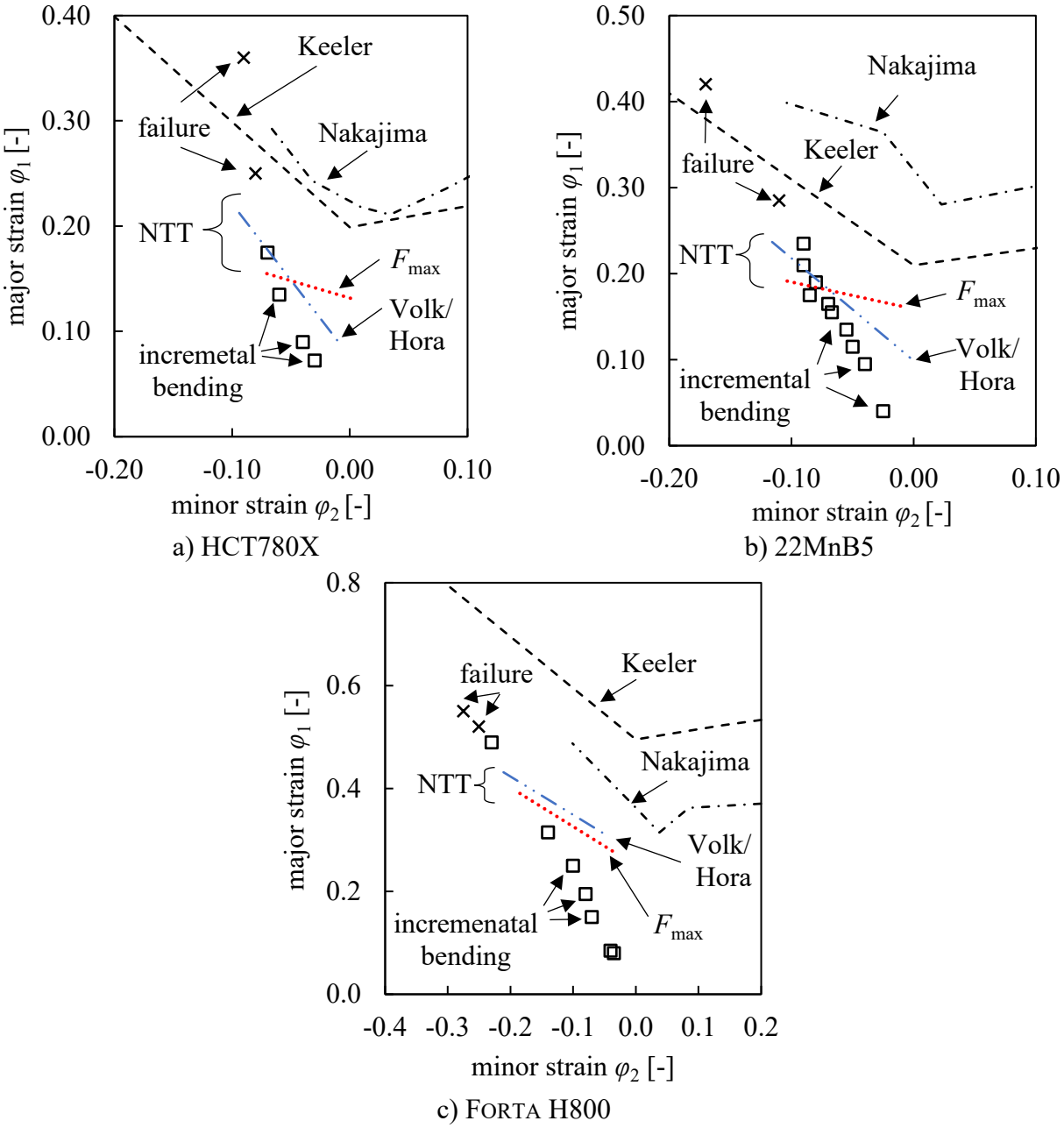

Figure 5: Comparison of experimental FLCs to strain maxima observed in incremental bending experiments and the FLC model of KEELER for three sheet metal materials. The measured FLCs were determined in NAKAJIMA experiments and by notched tension tests (NTT). Two methods for the evaluation of NTT FLCs are applied: force maximum F_{max} and strain rate fit according to Volk/Hora. Data points represent individual incremental bending experiments with successively increasing density according to Figure 4 right.

Two experimental FLCs are applied for prediction of failure. The NAKAJIMA testing method is a well-established tool in sheet metal forming. In addition, the failure curve is approximated by the results of the notched tension tests (NTT). Two evaluation methods for the corresponding FLCs are presented, one determining the beginning instabilities at force maximum and another using the method of bilinear approximation of strain rate according to VOLK & HORA [19]. With regard to the results from notched tension testing, the FLC obtained by the VOLK/HORA method resembles the inclination which usually obtained in the second quadrant of the FLD better than the method evaluating the force maximum. In addition, KEELER's semi-empirical modelling approach is compared for failure prediction. With regard to process setup, his FLC strongly resembles the experimentally determined NAKAJIMA FLCs because, originally, the coefficients of eq. (1) were fitted to deep drawing experiments by KEELER. The results of the incremental bending method represent successively increasing longitudinal strain with a free forming zone. The strain maxima at the bent extradoses are approximated with the least deviation by the VOLK/HORA approach based on NTT. For all materials, a slight underestimation of the forming potential remains which might be associated to the incremental nature of the conducted forming experiments. Similar deviations are only obtained by KEELER's approach, exclusively for 22MnB5, however by means of an overestimation of the material's forming potential.

Discussion and Conclusions

Because of the high variance observed from the modelling, testing and evaluation methods of the FLC, the application to any given forming process – in particular bending process, see [24 – 26] – needs to be considered. For example, for an application towards rotary draw bending (RDB) was conducted by KHODAYARI with the conclusion that in RDB the tubular material might even fail above the NAKAJIMA FLC [27]. For three point air bending, NEUHAUSER and TERRAZAS suggest to implement a third dimension to the FLD to capture the impact of bending strain on failure which underlines the relevance of these considerations [28]. However, compared to free form profile bending, a significant superposition of bending stress over sheet metal thickness ranging from full compression to full tension is present in over-thickness bending. In contrast, profile bending often features in-plane bending components. For incremental in-plane bending, a strong overestimation of the forming potential predicted by the Nakajima FLC is observed which is suspected due to the free forming zone that loses contact in force-fitted transmission of forming force [22]. Conclusively, it stays an open research question which FLC determination methodology might deliver the most reliable prediction for free-form bending.

In this regard, the notched tension tests (NTT) might deliver a better prediction because of the higher similarity to free-form bending. In contrast, three key differences towards the NAKAJIMA procedure are identified by the authors:

i) The of plane bending caused by the hemispherical punch of a NAKAJIMA assembly is absent in NTT,
ii) The blank surface is not impacted by friction shear stress, in particular during necking,
iii) Lack of heat transfer from blank towards tooling because no contact to any tooling is present in the deformation zone of NTT.

AFFRONTI & MERKLEIN investigated the influence of bending on the FLC [29]. The bending contribution was identified using FEM simulations of NAKAJIMA tests for different punch diameters. They were able to show that the influence of the bending strain only leads to deviations in the range of the standard deviation of the test repetitions. Therefore, it is assumed that the deviations of the FLC's observed in this work are not solely caused by bending over the hemispherical punch in the NAKAJIMA tests.

All these reasons might explain, why bending processes with shape related tooling and large contact zones, such as rotary draw bending show a better predictability by NAKAJIMA FLCs [5, 27]. The authors aim for applying the FLCs resulting from the herein presented notched tension tests to free form bending experiments to verify this assumption.

Technical standards and guidelines; sorted by type and number

DIN 50125	Prüfung metallischer Werkstoffe – Zugproben
DIN EN ISO 6892-1	Metallic materials – Tensile testing – Part 1: Method of test at room temperature
DIN EN ISO 12004-2	Metallic materials – Sheet and strip - Determination of forming-limit curves – Part 2: Determination of forming-limit curves in the laboratory

References

[1] R. Geiger *et al.*, *Lehrbuch der Umformtechnik: Band 3: Blechumformung*. Berlin, Heidelberg: Springer-Verlag, 2013.

[2] K. Siegert, *Blechumformung: Verfahren, Werkzeuge und Maschinen*. Berlin, Heidelberg: Springer-Verlag, 2015.

[3] K. Nakazima, T. Kikuma, and K. Hasuka, "Study on the formability of steel sheets," *Yawata technical report*, vol. 264, pp. 8517–8530, 1968.

[4] S. P. Keeler, "Plastic instability and fracture in sheets stretched over rigid punches," Dissertation, Massachusetts Institute of Technology, 1961.

[5] L. Borchmann, C. Kuhnhen, P. Frohn, and B. Engel, "Sensitivity analysis of the rotary draw bending process as a database of digital equipping support," *Procedia Manufacturing*, vol. 29, pp. 592–599, Jan. 2019, doi: 10.1016/j.promfg.2019.02.100.

[6] D. Y. Yang *et al.*, "Flexibility in metal forming," *CIRP Annals*, vol. 67, no. 2, Art. no. 2, Jan. 2018, doi: 10.1016/j.cirp.2018.05.004.

[7] C. Heftrich, R. Steinheimer, and B. Engel, "Rotary-draw-bending using tools with reduced geometries," *Procedia Manufacturing*, vol. 15, pp. 804–811, Jan. 2018, doi: 10.1016/j.promfg.2018.07.410.

[8] P. Frohn-Sörensen, B. Mašek, M. F.-X. Wagner, K. Rubešová, O. Khalaj, and B. Engel, "Flexible manufacturing chain with integrated incremental bending and Q-P heat treatment for on-demand production of AHSS safety parts," *Journal of Materials Processing Technology*, vol. 275, p. 116312, Jan. 2020, doi: 10.1016/j.jmatprotec.2019.116312.

[9] S. P. Keeler and W. G. Brazier, "Relationship between laboratory material characterization and press-shop formability," 1977.

[10] Z. Marciniak and K. Kuczyński, "Limit strains in the processes of stretch-forming sheet metal," *International Journal of Mechanical Sciences*, vol. 9, no. 9, pp. 609–620, Sep. 1967, doi: 10.1016/0020-7403(67)90066-5.

[11] P. Hora and L. Tong, "Theoretical prediction of the influence of curvature and thickness on the FLC by the enhanced modified maximum force criterion," in *Proceedings of the NUMISHEET 2008 Conference*, Interlaken, Switzerland, 2008, p. 7.

[12] D. Jocham, "Bestimmung der lokalen Einschnürung nach linearer und nichtlinearer Umformhistorie sowie Ermittlung dehnungs-und geschwindigkeitsabhängiger Materialkennwerte," PhD Thesis, Technische Universität München, 2018.

[13] S. P. Keeler, "Determination of Forming Limits in Automotive Stampings," *SAE Transactions*, vol. 74, pp. 1–9, 1966.

[14] C. D. Horvath, "2 - Advanced steels for lightweight automotive structures," in *Materials, Design and Manufacturing for Lightweight Vehicles*, P. K. Mallick, Ed. Woodhead Publishing, 2010, pp. 35–78. doi: 10.1533/9781845697822.1.35.

[15] S. K. Paul, "Controlling factors of forming limit curve: A review," *Advances in Industrial and Manufacturing Engineering*, vol. 2, p. 100033, May 2021, doi: 10.1016/j.aime.2021.100033.

[16] O. Selter, *Entwicklung der Verfahrenstechnik zum modularen Walzprofilierbiegen*, vol. 10. Dissertation, Aachen: Shaker Verlag GmbH, 2017.

[17] G. M. Goodwin, "Application of Strain Analysis to Sheet Metal Forming Problems in the Press Shop," SAE International, Warrendale, PA, SAE Technical Paper 680093, Feb. 1968. doi: 10.4271/680093.

[18] P. Brozzo, B. Deluca, and R. Rendina, “A new method for the prediction of formability limits in metal sheets,” 1972.
[19] W. Volk and P. Hora, “New algorithm for a robust user-independent evaluation of beginning instability for the experimental FLC determination,” *Int J Mater Form*, vol. 4, no. 3, pp. 339–346, Sep. 2011, doi: 10.1007/s12289-010-1012-9.
[20] A. Kuppert, *Erweiterung und Verbesserung von Versuchs-und Auswertetechniken für die Bestimmung von Grenzformänderungskurven*, vol. 267. Dissertation, Erlangen: Meisenbach, 2015. [Online]. Available: https://opus4.kobv.de/opus4-fau/frontdoor/index/index/docId/10485
[21] B. Engel, P. Frohn, M. Hillebrecht, and A. Knappe, “Incremental swivel bending for scalable lightweight structures,” *ATZ Worldw*, vol. 119, no. 5, Art. no. 5, May 2017, doi: 10.1007/s38311-017-0023-2.
[22] P. Frohn, L. Borchmann, and B. Engel, “On the forming mechanisms of frictionally engaged linear processes under consideration of incremental swivel bending (ISB),” *Procedia Manufacturing*, vol. 29, pp. 169–176, Jan. 2019, doi: 10.1016/j.promfg.2019.02.122.
[23] P. Frohn-Sörensen, C. Cislo, H. Paschke, M. Stockinger, and B. Engel, “Dry friction under pressure variation of PACVD TiN surfaces on selected automotive sheet metals for the application in unlubricated metal forming,” *Wear*, vol. 476, p. 203750, Jul. 2021, doi: 10.1016/j.wear.2021.203750.
[24] S. Groth, P. Frohn, and B. Engel, “Product planning system for manufacture-oriented modeling of freeform bend tubes produced by three-roll-push-bending,” *Procedia Manufacturing*, vol. 34, pp. 10–18, Jan. 2019, doi: 10.1016/j.promfg.2019.06.107.
[25] B. Engel, S. Kersten, and D. Anders, “Spline-Interpolation and Calculation of Machine Parameters for the Three-Roll-Pushbending of Spline-Contours,” *steel research international*, vol. 82, no. 10, Art. no. 10, 2011.
[26] M. Hermes, D. Staupendahl, C. Becker, and A. E. Tekkaya, “Innovative Machine Concepts for 3D Bending of Tubes and Profiles,” *Key Engineering Materials*, 2011. https://www.scientific.net/KEM.473.37 (accessed Oct. 24, 2019).
[27] G. Khodayari, “Bending Limit Curve for Rotary Draw Bending of Tubular Components in Automotive Hydroforming Applications,” *SAE International Journal of Materials and Manufacturing*, vol. 1, no. 1, pp. 841–848, 2009.
[28] F. M. Neuhauser, O. Terrazas, N. Manopulo, P. Hora, and C. Van Tyne, “The bending dependency of forming limit diagrams,” *Int J Mater Form*, vol. 12, no. 5, pp. 815–825, Sep. 2019, doi: 10.1007/s12289-018-1452-1.
[29] E. Affronti and M. Merklein, “Analysis of the bending effects and the biaxial pre-straining in sheet metal stretch forming processes for the determination of the forming limits,” *International Journal of Mechanical Sciences*, vol. 138–139, pp. 295–309, Apr. 2018, doi: 10.1016/j.ijmecsci.2018.02.024.